Springer

Journal of Mechanical Science and Technology 23 (2009) 461~474

Journal of Mechanical Science and Technology

www.springerlink.com/content/1738-494x
DOI 10.1007/s12206-008-1127-9

# Upper bound analysis of extrusion from square billets through circular and square/rectangular dies †

Joseph S. Ajiboye*

*Department of Mechanical Engineering, University of Lagos, Lagos, Nigeria*

(Manuscript Received May 26, 2008; Revised November 23, 2008; Accepted November 26, 2008)

**Abstract**

Upper bound elemental technique (UBET) for prediction of extrusion pressure in three-dimensional forward extrusion process is presented. Using square/rectangular billets, the study of the effect of die land length has been extended for the evaluations of extrusion pressures to extrude sections such as circular, square and rectangular shaped sections with power of deformation due to ironing effect at the die land taken into account. The extrusion pressure contributions due to the die land evaluated theoretically for these shaped sections considered are found to increase with die land lengths for any given percentage reduction and also increase with increasing percentage die reductions at any given die land length. The effect of die land lengths on the extrusion pressures increases with increasing complexity of die openings geometry with rectangular section giving the highest extrusion pressure followed by circular with square section die opening, giving the least extrusion pressure for any given die reduction at any given die land lengths. The proper choice of die land length is imperative if excessive pressure buildup at the emergent section is to be avoided so as to maintain good quality and metallurgical structure of the extrudates.

*Keywords*: Die land; Die opening geometry; Extrusion pressures; Percentage reduction in area; 3-D Upper bound

## 1. Introduction

Upper bound analysis of three-dimensional metal forming processes in general and extrusion in particular has remained a subject of continuum focus of study due to its high productivity, lower cost and increased properties. However, the process itself is difficult to analyze due to the unpredictable behavior of metal flow during extrusion. There are several analytical approaches available to metal forming problems, including slip-line field theory, upper bound and lower bound analyses and finite element methods. The slip-line approach has been employed successfully only in analyzing plane-strain problems.

On the other hand, finite element methods (FEM) have recently found much favour and are now increasingly being applied to many metal forming problems. Although the FEM provides a more accurate description of the deformation and stresses than do other methods, it demands an expert's use of a considerable amount of computer time. The upper bound approach has much to recommend it, since, it is simple, takes less computer time and expertise, and the results obtained are within reasonable engineering approximations. As regards the three-dimensional extrusion of shaped sections, some analytical methods for predicting the metal flow according to the optimum die configurations have been proposed by some workers [1-5]. Yang and Lee [6] proposed an energy method for analysis of three-dimensional sheet metal forming of noncircular cups with complicated shape. They expressed the geometric shape and velocity fields by, respectively, sweeping the section curves defined on the boundary of each zone and velocity

† This paper was recommended for publication in revised form by Associate Editor Youngseog Lee

*Corresponding author. Tel.: +82 10 2232 3267
E-mail address: joesehinde@yahoo.com

functions. Nagpal and Altan [7] proposed dual stream functions to obtain a kinematically admissible velocity field that demonstrated a three-dimensional metal flow. Their model, however, was limited to the extrusion of ellipse bar or rod.

Yang and Lee [8] adopted a conformal mapping approach to obtain a velocity field for extrusion through concave and convex-shaped dies where geometrical similarity is preserved throughout the deformation. The axial velocity in their study was kept uniform at any cross-section. Wu and Hsu [9] employed the upper bound method, as well as a three-dimensional velocity field which has a non-uniform velocity distribution along the extrusion axis and a non-linear variation velocity component along the radius to extrude a composite rod. All their three-dimensional velocity fields of sleeve and core were generated with the aid of the shape of the final product. The composite rod billets they used are non-axisymmetric cross-sectional profiles like rectangular, hexagonal and octagonal sections which are examined. Three-dimensional extrusion is not limited to direct extrusion processes alone. Bae and Yang [10] proposed a simple kinematically admissible velocity field for the three-dimensional deformation, from which the upper bound extrusion load, the velocity distribution, and the configuration of the extruded billet are determined by minimizing the total power consumption with respect to chosen parameters. Nagpal [11] proposed an analytical method for the extrusion of tubes of elliptic internal shapes from round billets using dual stream functions. Yang and Han [12] analyzed three-dimensional backward extrusion using conformal transformation: theoretical results were in good agreement with those from experiment, but the formulation is rather complex and the computation time needs to be reduced considerably for easier design of more complicated backward-extrusion processes. The analyses were confined to just the steady-state condition of the process, so that there is the need of a method, such as the upper-bound method, to obtain a simple velocity field to solve both the non-steady state and the steady state within a reasonably reduced computation time. Kim and Park [13] proposed a kinematically admissible velocity field for torsional backward extrusion by using stream function. Kim et al studied the torsional forging process [14-16]. Gatto and Giarda [17] proposed a method for constructing kinematically admissible discontinuous velocity fields for upper bound analysis of three-dimensional plastic deformation problems termed spatial elementary rigid regions (SERR) which is a generalization of the planar elementary rigid regions (PERR) method devised to analyze plane strain deformation problem. Their formulation appears to be unsuitable for analyzing extrusion processes when the product and the billet have different sections, especially when the product section has re-entrant corners. Kar and Das [18] reformulated the SERR technique so that it could be applied to analyze extrusion of bars of any cross section from billets of any other cross section when the product and billet boundaries were defined by planar surfaces. All the above mentioned authors limited their working materials to round billets except Kar and Das and all excluded die land or straight portion of die. The effect of percentage reduction in area and the die land length is seen to be more pronounced experimentally in I-shaped sections than in T-shaped sections. Chitkara and Adeyemi [19] investigated the effect of percentage reduction in area on the extrusion pressures of I and T-shaped die openings with extrusion pressures of I-shaped section being higher than for T-shaped section opening. Yang [20] derived a theoretical equation for rod drawing operations that included the effect of the land and compared the values of friction coefficients from both calculations; including and neglecting die land. The differences between the friction coefficients calculated with and without the land were found to be appreciable and hence suggested the inclusion of die land effects in both the theoretical and experimental analyses. Kiuchi et al [21] developed an upper bound based analytical method to calculate power requirements, the extrusion pressure, the optimal die length in extruding/drawing from round, square and rectangular billets to rods, bars and wires with square, rectangular, hexagonal, L-type, T-type, H-type and flower-type cross-sections. For this generalized formulation, it also has a setback for neglecting to account for the frictional forces at the die land region. Nanhai et al [22] stressed the importance of proper simulation of die land in the extrusion of shapes with flat-faced die so as to avoid the generations of geometrical defects and hence proposed a method of simulation, using finite element method, that the metal flow in extrusion and the die land can be adjusted according to the simulation results. Ajiboye and Adeyemi [23] improved on Kiuchi et al's formulations [21] to account for power losses due to ironing effect at the die land of an extrusion die with circular

die opening. Their investigations involved the determinations of both experimental and theoretical effects of die land lengths on the quality of extruded products, extrusion pressures and flow patterns of cold-extruded lead alloy of circular sections Avitzur [24] gave a detailed theoretical formulation which accounted for the power losses due to friction between the die land and round billets during drawing and extrusion processes to smaller rod products. He concluded that an increase in die land led to an increase in the required force and a decrease in maximum possible reductions. Ajiboye and Adeyemi [25] extended their study on the upper bound method of analysis of the effects of die land lengths on the extrusion pressures to complex extruded sections such as square, rectangular, I- and T-shaped sections from initially round billets with the powers of deformations due to ironing effect at die land taken into account. Chitkara and Celik [26] developed, based on upper bound theory, a three-dimensional extrusion of non-symmetric T-shaped sections from initially round billets. There is, to the best of author's knowledge, no research work so far that has either been presented or done on the three-dimensional extrusion of shaped section using UBET with the powers of deformations due to ironing effect at die land taken into account.

In the present study, the previously two-dimensional polar coordinates analytical approach (Int. J. Mech. Sci. 49 (2007) 335 – 351), based on the upper-bound theory was replaced with a more generalized three-dimensional formulation of the UBET. The three-dimensional analysis for the extrusion of circular and square/rectangular from initially square/rectangular billets is studied and presented. The contents are divided into two major parts: flow pattern and energy rates. The first part presents the formulation of velocity field equations and their associated strain rate fields. The second part discusses the computation of energy rates coupled with optimizing algorithms for the inherent velocity fields during the assemblage of elements. The effect of the die land length, die opening profiles and percentages reductions in areas on the extrusion pressure contributions due to die land effects are also investigated theoretically and presented.

## 2. Theoretical analysis

### *2.1 Shape and dimension of die surface*

Figs. 1(a) and 1(b) respectively show the schematic diagrams of the die surface and shape plus dimensions of the linearly converging die, in Cartesian coordinates system used for the present numerical calculations. In the present modeling, the surface in Cartesian coordinates is represented by $z_s(x, y)$. The die surface [21] is derived by using linearly converging straight lines as:

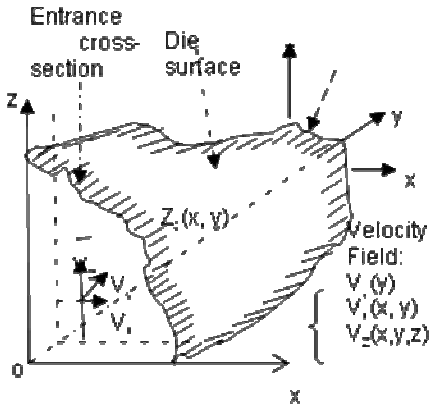


Fig. 1(a). Schematic diagram of the die surface in Cartesian coordinate system.

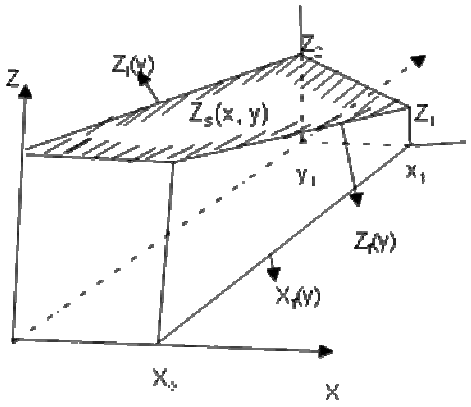


Fig. 1(b). Shape and dimensions of linearly converging die.

$$z_s(x,y) = \frac{z_f(y) - z_i(y)}{x_f(y)} x + z_i(y) \tag{1}$$

where $z_f(y) = (z_i - z_o)\dfrac{y}{y_1} + z_o$

$$z_i(y) = (z_2 - z_o)\frac{y}{y_1} + z_o$$

$$x_f(y) = (x_i - x_o)\frac{y}{y_1} + x_o$$

where $x_1$, $x_o$ and $z_i$, $z_o$ are the dimensions of die and billet respectively and $y_1$ is the length of the die. By using Eq. (1), and the function $z_s$,(x, y) all of the strain rate components and the total powers of deformation can be calculated.

The boundary limits for the die surfaces are

$$\begin{aligned} &0 \le x \le x_f(y) \\ &0 \le z \le z_s(x,y) \\ &0 \le y \le y_1 \end{aligned} \tag{2}$$

### *2.2 Assumptions and velocity fields*

The following assumptions [25] are used;

i) the longitudinal velocity, $V_y$, is uniform at each cross-section of the material in the die and is equal to inlet velocity denoted by $V_o$ at the entry.

ii) The von-Mises yield criterion is assumed to be applicable.

The generalized formulas of the kinematically admissible velocity field can be formulated as follows. At first, the condition of volume constancy may be expressed as

$$\dot{\varepsilon}_x + \dot{\varepsilon}_y + \dot{\varepsilon}_z = 0 \tag{3}$$

that is,

$$\frac{\partial}{\partial x}V_x(x,y,z) + \frac{\partial}{\partial y}V_y(x,y,z) + \frac{\partial}{\partial z}V_z(x,y,z) = 0 \tag{4}$$

Assuming that the longitudinal velocity component $V_y$ is uniform at every cross-section of the material, $V_y$ is derived as follows:

From continuity equation, i.e., $VA = V_oA_o$, we have

$$V_y(y)\int_0^{x_f(y)} z_s(x,y)dx = V_o\int_0^{x_f(0)} z_s(x,0)dx$$

from where

$$V_y(y) = \frac{V_o\int_0^{x_f(0)} z_s(x,0)dx}{\int_0^{x_f(y)} z_s(x,y)dx} \tag{5}$$

Using Eq. (5) in Eq. (4) gives

$$\frac{\partial}{\partial x}V_x(x,y,z) + \frac{\partial}{\partial y}V_y(y) + \frac{\partial}{\partial z}V_z(x,y,z) = 0$$

from where

$$\frac{\partial}{\partial z}V_z(x,y,z) = -\frac{\partial}{\partial y}V_y(y) - \frac{\partial}{\partial x}V_x(x,y,z)$$

which upon integrating we have

$$V_z(x,y,z) = -\int_0^z \left[\frac{\partial}{\partial x}V_x(x,y,z) + \frac{\partial}{\partial y}V_y(y)\right]dz \tag{6}$$

Eq. (6) satisfies the boundary condition of $V_z$(x, y, z), i.e., when z = 0, $V_z$(x, y, 0) = 0. From the boundary condition that the material should flow along the shape of the die surface we have,

$$\begin{aligned} V_z(x,y,z_s(x,y)) &= -V_x(x,y,z_s(x,y))\frac{\partial}{\partial x}z_s(x,y) \\ &\quad - V_y(y)\frac{\partial}{\partial y}z_s(x,y) \\ &= -\int_0^{z_s(x,y)}\left\{\frac{\partial}{\partial x}V_x(x,y,z) + \frac{\partial}{\partial y}V_y(y)\right\}dz \end{aligned} \tag{7}$$

Treating the derivatives of x and y in Eq. (7) as a constant, $V_z$(x, y, $z_s$(x, y)) will be zero and hence (7) reduces to

$$\frac{\partial}{\partial x}\int_0^{z_s(x,y)} V_x(x,y,z)dz + \frac{\partial}{\partial y}\int_0^{z_s(x,y)} V_y(y)dz = 0 \tag{8}$$

If the velocity component $V_x$ is a function of x, y and z, Eq. (8) cannot be solved any more. Therefore the following assumption is employed: $V_x$ is a function of x, and y only. Introducing this assumption and integrating Eq. (8), Vx is expressed as

$$\frac{\partial}{\partial x}\left[V_x(x,y).z_s(x,y)\right] = -\frac{\partial}{\partial y}\left[V_y(y).z_s(x,y)\right]$$

from where

$$V_x(x,y).z_s(x,y) = -\int_0^x \frac{\partial}{\partial y}V_y(y).z_s(x,y)dx$$

and the velocity component along x-axis will be given as

$$V_x(x,y) = \frac{-1}{z_s(x,y)}\int_0^x \frac{\partial}{\partial y}\left[V_y(y).z_s(x,y)\right]dx \tag{9}$$

Eq. (9) satisfies the boundary condition of $V_x(x, y)$ i.e. when x = 0, $V_x(0, y) = 0$. Taking the assumption that $V_x$ is a function of x and y into consideration, Eq. (4) is reduced to

$$V_z(x,y,z) = -\int_0^z \left[\frac{\partial}{\partial x}V_x(x,y) + \frac{\partial}{\partial y}V_y(y)\right]dz = -z\left[\frac{\partial}{\partial x}V_x(x,y) + \frac{\partial}{\partial y}V_y(y)\right] \tag{10}$$

Now on the die surface, where $z = z_s(x, y)$, Eq (10) becomes

$$V_z(x,y,z_s(x,y)) = -z_s(x,y)\left[\frac{\partial}{\partial x}V_x(x,y) + \frac{\partial}{\partial y}V_y(y)\right] \tag{11}$$

From Eq. (9), we have by differentiation using the product rule as

$$\frac{\partial}{\partial x}V_x(x,y).z_s(x,y) + V_x(x,y).\frac{\partial}{\partial x}z_s(x,y) = -\frac{\partial}{\partial y}V_y(y).z_s(x,y) - V_y(y).\frac{\partial}{\partial y}z_s(x,y) \tag{12a}$$

Solving for the derivative of the velocity $V_x(x, y)$, gives

$$\frac{\partial}{\partial x}V_x(x,y) = \frac{-1}{z_s(x,y)}.\frac{\partial}{\partial x}z_s(x,y).V_x(x,y) - \frac{\partial}{\partial y}V_y(y) - \frac{-1}{z_s(x,y)}.V_y(y).\frac{\partial}{\partial y}z_s(x,y) \tag{12b}$$

Substituting Eq. 12(b) into Eq. (11) to give

$$V_z(x,y,z_s(x,y)) = -z_s(x,y)\left[\begin{array}{l}\frac{-1}{z_s(x,y)}.\frac{\partial}{\partial x}z_s(x,y)..V_x(x,y) - \frac{\partial}{\partial y}V_y(y) \\ \qquad - \frac{1}{z_s(x,y)}.V_y(y).\frac{\partial}{\partial y}z_s(x,y) \\ \qquad + \frac{\partial}{\partial y}V_y(y)\end{array}\right]$$

Opening the brackets this reduces to

$$V_z(x,y,z_s(x,y)) = \frac{\partial}{\partial x}z_s(x,y).V_x(x,y) + \frac{\partial}{\partial y}z_s(x,y).V_y(y) \tag{13}$$

Eq. (13) means that the material on the die surface flows along the shape of the die. This is the boundary condition for the metal flow on the die surface. Eqs. (5), (9) and (10) are called the kinematically admissible velocity field which satisfies the condition of volume constancy and all of the kinematic boundary conditions.

The formulae of the velocity field derived through the above mentioned procedures are based upon the functions expressing the shapes of employed die, given by Eq. (1). Therefore, when these functions are given, even if they have complicated three-dimensional geometry or forms, the velocity field is easily calculated. These formulae of the velocity fields can be applied to solve extrusion processes.

### *2.3 Strain rate components*

The strain rate components are the derivatives of kinematically admissible velocity fields of Eqs. (5), (9) and (10). Now, differentiating velocity Eq. (9) to get strain rate along x-axis,

$$\dot{\epsilon}_{xx}(x,y) = \frac{\partial}{\partial x}V_x(x,y) = -\frac{\frac{\partial}{\partial x}z_s(x,y)}{z_s(x,y)}.V_x(x,y) - \frac{\partial}{\partial y}V_y(y) - \frac{\frac{\partial}{\partial y}z_s(x,y)}{z_s(x,y)}.V_y(y) \tag{14}$$

The strain rate components along the y-axis are obtained by differentiating the kinematically admissible velocity field Eq. (5):

$$\dot{\epsilon}_{yy}(y) = \frac{\partial}{\partial y}V_y(y) = -V_o\int_0^{x_f(0)} z_s(x,y)dx\ \ x \cdot \frac{z_s(x_f(y),y).\frac{\partial}{\partial y}x_f(y) + \int_0^{x_f(y)}\frac{\partial}{\partial y}z_s(x,y)}{\left[\int_0^{x_f(y)} z_s(x,y)dx\right]^2}dy \tag{15}$$

From Eqs. (14) and (15), the strain $\in_{zz}(x,y)$ is obtained as:

$$\dot{\epsilon}_{zz}(x,y) = -\left[\frac{\partial}{\partial x}V_x(x,y) + \frac{\partial}{\partial y}V_y(y)\right] \tag{16}$$

The other components of strain rates are defined as follows;

$$\in_{zx}(x,y,z) = -\frac{-z}{2}.\frac{\partial^2}{\partial x^2}V_x(x,y) \tag{17}$$

$$\in_{xy}(x,y) = \frac{1}{2}.\frac{\partial}{\partial y}V_x(x,y) \tag{18}$$

$$\in_{yz}(x,y,z) = \frac{-z}{2}\left[\begin{array}{c}\frac{\partial^2}{\partial y \partial x}V_x(x,y) \\ + \frac{\partial^2}{\partial y^2}V_y(y)\end{array}\right] \tag{19}$$

## 3. The upper bound solution

The total power consumption, $J^*$, during extrusion through the die is the sum of the power losses due to the plastic deformation inside the die, ($E_i$), due to velocity discontinuities at entry, exit and when the profiles of the entrance and exit cross-sections of the material have singular points: the planes including a singular point and the longitudinal axis are also defined as the boundaries of velocity discontinuity, ($E_s$), and that due to frictional resistance at the interface between the material and the die, ($E_f$). The upper bound on total power dissipated is expressed as the sum of the individual terms for internal power, shear power and the power to overcome prescribed surface tractions. Each of these individual contributions will now be computed separately.

$$J^* = \dot{E}_i + \sum_n \dot{E}_s + \sum_k \dot{E}_f \tag{20}$$

The total will be calculated and a minimization procedure will be performed on the upper bound to obtain the extrusion pressure to extrusion process.

The individual power loss components are evaluated as follows.

### *3.1 The internal power of deformation;*

$$E_i = \frac{2\bar{\sigma}_m}{\sqrt{3}}\iiint_v \sqrt{\frac{1}{2}\dot{\varepsilon}_{ij}\dot{\varepsilon}_{ij}}dV \ ,$$

The first term on the right-hand side of Eq. (20) represents the internal power of deformation $E_i$. The internal power of deformation can be calculated by:

$$\dot{E}_i = \sigma_o \iiint \sqrt{\frac{2}{3}\left\{\begin{array}{c}\dot{\in}_{xx}^2 + \dot{\in}_{yy}^2 + \dot{\in}_{zz}^2 \\ + 2\left(\dot{\in}_{xy}^2 + \dot{\in}_{yz}^2 + \dot{\in}_{zx}^2\right)\end{array}\right\}}\Delta V \tag{21a}$$

i.e.

$$\dot{E}_i = \sigma_o \iiint \sqrt{\frac{2}{3}\left\{\begin{array}{c}\dot{\in}_{xx}^2 + \dot{\in}_{yy}^2 + \dot{\in}_{zz}^2 \\ + 2\left(\dot{\in}_{xy}^2 + \dot{\in}_{yz}^2 + \dot{\in}_{zx}^2\right)\end{array}\right\}}dxdydz \tag{21b}$$

### *3.2 Shear power*

The second term on the right-hand side of Eq. (20) accounts for the shear losses along surfaces of velocity discontinuity. The power of deformation due to shear loss $E_s$ is given [1] as:

$$\dot{E}_s = \int_{\Gamma_s} \frac{\sigma_o}{\sqrt{3}}(\Delta V)_{\Gamma_s} dS \tag{22}$$

where

$$(\Delta V)_{\Gamma_s} = \sqrt{V_x^2(x,y^*) + V_z^2(x,y^*,z)}$$

where $\Gamma_s$ are the boundaries of velocity at entrance and exit and internal boundaries of discontinuity due to the singular points on the profile at entrance and exit of cross-sections and dS is the elemental surface area; $y^*$ is the y-coordinate denoting the entrance and exit. The relative slip on the internal boundaries at singular points on profile is calculated by

$$(\Delta V)_{\Gamma_s} = \left[\begin{array}{c}V_z(x^* + 0, y, z) \\ - V_z(x^* - 0, y, z)\end{array}\right] \tag{23}$$

where $x^* + 0$, $x^* - 0$ denote co-ordinates of the slip-line boundaries.

The calculation is simplified when the discontinuity planes are normal to the axes. For a Cartesian system with x, y and z coordinates, the directions of the three possible discontinuity planes coincide with those of the coordinate system, as given below.

For shear plane normal to x-axis, i.e. y axis is normal to this plane, x-axis then the velocity difference is given as

$$\left|\Delta u_{(x=x_s)}\right| = \left[\sqrt{\left\{\begin{array}{c}(V_y^i(x,y) - V_y^j(x,y))^2 + \\ (V_z^i(x,y,z) - \\ V_z^j(x,y,z))^2\end{array}\right\}}dydz\right]$$

where the superscripts i and j refer to elements i and j, respectively. Thus the shear loss using Eq. (22) is

$$\dot{E}_{sx} = \int_{z=0}^{\gamma}\int_{y=0}^{\beta}\left[\sqrt{\begin{array}{l}((V_y^i(x,y)\\ -V_y^j(x,y))^2\\ +(V_z^i(x,y,z)\\ -V_z^j(x,y,z))^2\end{array}}\right]_{x=x_o} dydz \qquad (24)$$

The limits of integration β and γ depend on the geometry of the shear area. For a rectangle, we must have β = b and γ = c.

Similarly, when the shear surface is normal to the y axis, the expression for shear power is

$$\dot{E}_{sy} = \int_{z=0}^{\gamma}\int_{x=0}^{\alpha}\left[\sqrt{\begin{array}{l}(V_z^i(x,y,z)\\ -V_z^j(x,y,z))^2\\ +(V_x^i(x,y)\\ -V_x^j(x,y))^2\end{array}}\right]_{y=y_s} dxdz \qquad (25)$$

The limits of integration are γ = c and α = a for the rectangle.

Finally, for the shear loss when the shear plane is normal to the z axis, the equation for shear loss is

$$\dot{E}_{sz} = \int_{y=0}^{\beta}\int_{x=0}^{\alpha}\left[\sqrt{\begin{array}{l}(V_x^i(x,y)\\ -V_x^j(x,y))^2\\ +(V_y^i(y)\\ -V_y^j(y))^2\end{array}}\right] dxdy \qquad (26)$$

with β = b and α = a for rectangular surface.

#### *3.2.1 Shear power losses at singular points of profiles*

When the extruded product involves singularities in the form of re-entrant corners (such as square, rectangular, I- and T-section), the shear losses at these singularities points in rectangular and square geometries can be obtained as

$$\dot{E}_s = 4\int_{\Gamma_s}\frac{\sigma_o}{\sqrt{3}}(\Delta V)_{\Gamma_s}\, dS \qquad (27)$$

where

$$(\Delta V)_{\Gamma_s} = \left[V_z\left(x^* + 0, y, z\right) - V_z\left(x^* - 0, y, z\right)\right]$$

For T-section, Eq. (27) can be modified to obtain the shear losses at singular points as

$$\dot{E}_s = 8\int_{\Gamma_s}\frac{\sigma_o}{\sqrt{3}}(\Delta V)_{\Gamma_s}\, dS \qquad (28)$$

where

$$(\Delta V)_{\Gamma_s} = \left[V_z\left(x^* + 0, y, z\right) - V_z\left(x^* - 0, y, z\right)\right]$$

While for that of the I-section, Eq. (28) can be modified to obtain the shear losses at singular points as

$$\dot{E}_s = 12\int_{\Gamma_s}\frac{\sigma_o}{\sqrt{3}}(\Delta V)_{\Gamma_s}\, dS \qquad (29)$$

where

$$(\Delta V)_{\Gamma_s} = \left[V_z\left(x^* + 0, y, z\right) - V_z\left(x^* - 0, y, z\right)\right]$$

### *3.3 Frictional power losses at surfaces:*

The friction power equation is given as:

$$\int_S \tau|\Delta u| dS \qquad (30)$$

where

$$|\Delta u| = \sqrt{V_y^2(y) + V_x^2(x,y) + V_z^2(x,y,z)}$$

and Δu denotes the resultant velocity along surfaces S, Γ is the tractive shear stress, dS is the elemental element taken on the surface S, $z = z_o(x, y)$.

#### *3.3.1 Frictional power loss along the die surface*

The friction power loss along the die surface is given as, using Eq. (26),

$$\dot{E}_{f_{die}} = \frac{m\sigma_o}{\sqrt{3}}\iint_{R^*}\sqrt{\begin{array}{l}\{V_y^2(y) + V_x^2(x,y)\\ +V_z^2(x,y,z_s(x,y))\}\end{array}} dS \qquad (31)$$

$R^*$ is the projection of S onto the xy plane, m is the friction coefficient

The surface is explicitly given as

$$z_s(x,y) = \frac{(m_3 - m_2)}{m_1 y + x_o}xy + m_2 y + z_o \qquad (32)$$

where,

$$m_1 = \frac{x_1 - x_o}{y_1};\ m_2 = \frac{z_2 - z_o}{y_1};\ m_3 = \frac{z_1 - z_o}{y_1};$$
$$dS = \sqrt{1 + \left(\frac{\partial z_s}{\partial x}\right)^2 + \left(\frac{\partial z_s}{\partial y}\right)^2}\, dxdy \tag{33}$$

### 3.3.2 Frictional power at workpiece-punch interface

The frictional power dissipated at the work material/punch interface is given as

$$\dot{E}_{m/p} = \frac{m\sigma_o}{\sqrt{3}} \int_0^{\gamma} \int_0^{\beta} \left|V_z(x,y,z)\right| dxdy;$$

where

$$V_z(x,y,z) = -z\left[\frac{\partial}{\partial x} V_x(x,y) + \frac{\partial}{\partial y} V_y(y)\right] \tag{34}$$

From the assumption that the axial velocity component $V_y$ is uniform at each cross-section of the material in the die, using the compressibility condition, the volume of material displaced in unit time due to the descent of the top die at velocity $V_o$ is $A_oV_o$. The loss of material from this inlet zone into the exit zone is equal to the gain of material from the inlet zone, since the metal is incompressible. This is given by the product of the exit velocity $V_y(y)$ and exit area, $A_yV_y(y)$.

$$V_y(y) = \frac{y}{H_o - y'}\left(\frac{V_o A_o}{A_y}\right) = \frac{y}{H_o - y'} \cdot \frac{V_o \int_0^{x_f(0)} z_s(x,y)dx}{\int_0^{x_f(y)} z_s(x,y)dx} \tag{35}$$

where $y'$ is the current billet height to die surface and $H_o$ is the original billet height.

### 3.3.3 Frictional power at the container/billet interface

The frictional power at the billet/container interface is due to the axial sliding velocity between the moving billet and stationary die. Integrating over the channel $(H_o - y')$, we have

$$\dot{E}_{b/c} = \frac{2m\sigma_o}{\sqrt{3}}\left[\int_0^{(H_o - y')} \int_0^{\alpha} \left|V_y(y)\right| dxdz + \int_0^{(H_o - y')} \int_0^{b} \left|V_y(y)\right| dzdy\right] \tag{36}$$

### 3.3.4 Frictional power at die land

The present formulation based on upper bound analysis accounts for frictional power at the die land due to ironing effect. The axial velocity is modified, by using the condition of volume constancy between the inlet and the die land region as follows:

$$\dot{E}_{land} = \frac{2m\sigma_o}{\sqrt{3}}\left[\int_0^{a} \int_0^{l} \left|V_y(y)\right| dydz + \int_0^{b} \int_0^{l} \left|V_y(y)\right| dxdz\right] \tag{37}$$

where l is the die land length, a and b are die opening section lengths in x and y axes and

$$V_y(y) = \frac{y}{H_o - y'} \cdot \frac{V_o \int_0^{x_f(0)} z_s(x,y)dx}{\int_0^{x_f(y)} z_s(x,y)dx}$$

Using square billets, the frictional powers at the die land region, for circular and shaped sections, such as rectangular and square are evaluated from expressions such as:

i) For rectangular section of sides 2a and 2b

$$E_{f_{land}} = \frac{2m\sigma_o}{\sqrt{3}}\left[\int_0^{2a} \int_0^{l} V_y(y)dydz + \int_0^{2b} \int_0^{l} V_y(y)dxdz\right] \tag{38}$$

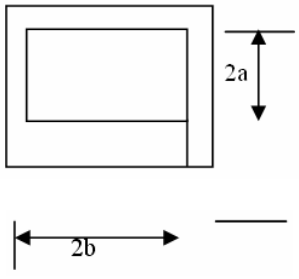


Fig. 2. Rectangular die opening.

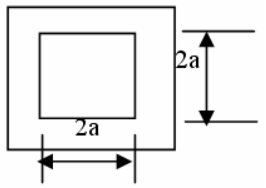


Fig. 3. Square die opening.

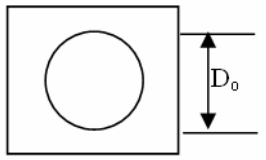


Fig. 4. Circular die opening.

ii) For square section of sides 2a

$$\dot{E}_{land} = \frac{4m\sigma_o}{\sqrt{3}}\left[\int_0^{2a}\int_0^{l} V_y(y)dydz\right] \tag{39}$$

iii) For circular die opening of perimeter $2\pi r_o$ where $r_o$ is the radius of circle,

$$\dot{E}_{f_{land}} = \frac{m\sigma_o}{\sqrt{3}}\int_0^{l}\int_0^{2\pi r_o} V_y(y)dydz \tag{40}$$

Therefore, the total frictional power $\sum W_f$ is given by

$$\sum W_f = W_{f_1} + W_{f_2} + W_{f_{land}} \tag{41}$$

Therefore, the total powers of deformation, $J^*$ is obtained, using

$$J^* = W_i + \sum W_s + \sum W_f \tag{42}$$

The power computed was converted to dimensionless parameter as follows:

The dimensionless extrusion pressure $\frac{P}{\sigma_0}$ is given by

$$\frac{P}{\sigma_0} = \frac{P^*}{A_0 V_0 \sigma_o} \tag{43}$$

The die land length (x) is also reduced to the relative die land length by dividing by original billet height ($x/H_o$).

## 4. Computational method

When the geometry of exit cross –section or the die is given, the surface of the die can then be known explicitly. By performing, the necessary differentiations and integrations on shapes of the die surface functions, the velocity field Eqs. (5), (9) and (10) and strain rates Eqs. (14)-(19) were derived.

The area and volume integrals of Eq. (42) were performed, by using the Gaussian quadrature integration techniques by transforming the polynomial variable by:

$$\phi(x_i) = \frac{(b-a)z_i + (b-a)}{2} \tag{44}$$

where a and b are respectively the upper and lower limits of integrations of the zone of die surface giving.

The area integrals of the friction losses, $W_f$, *and* shear losses, $W_s$,

$$\int\int \psi(\eta,\varepsilon)d\eta d\varepsilon = \sum_{1=1}\sum_{j=i} W_p\, W_j\, \psi(\eta_i,\varepsilon_j)d\eta d\varepsilon \tag{45}$$

where $\psi(\eta_i\varepsilon_j)$ is the resultant velocity field and $W_p$ $W_j$ are assigned weightings and for volume integrals of the internal powers of deformation ($W_i$) given as

$$\iiint \psi(\eta,\varepsilon,G)d\eta d\varepsilon dG = \sum_{i=1}\sum_{j=1}\sum_{k=1}\psi(\eta_{i,}\varepsilon_{j,}G_k)dv \tag{46}$$

where $\psi(\eta_i,\varepsilon_j,G_k)$ is the resultant strain and volume under deformation. A computer program written in C++ language was used [23] to evaluate various components of Eq. (42) to determine dimensionless extrusion pressure.

## 5. Results and discussion

### *5.1 Relative extrusion pressure, (P/Y), determinations*

#### *5.1.1 Rectangular, square and circular die openings*

The relative extrusion pressures, P/Y, versus relative die lengths, $l/X_o$, for circular, square and rectangular (b:a = 2:1) sections are shown in Figs. 5, 6 and 7 respectively, for varying die land lengths indicated. For a given die land length, x, the relative extrusion pressures, P/Y, decrease with increasing relative die lengths, $l/x_o$, until a minimum relative length is

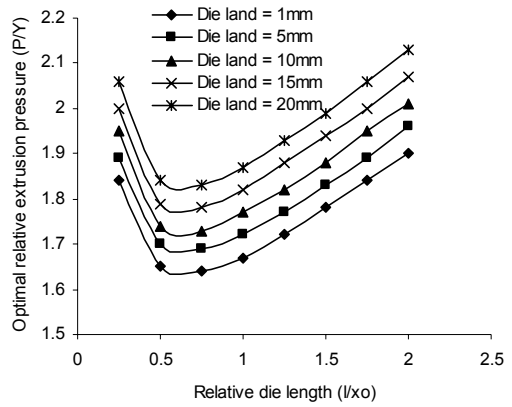


Fig. 5. Effects of die land lengths on the extrusion pressures of circular die opening at a given die reduction in area of 58%.

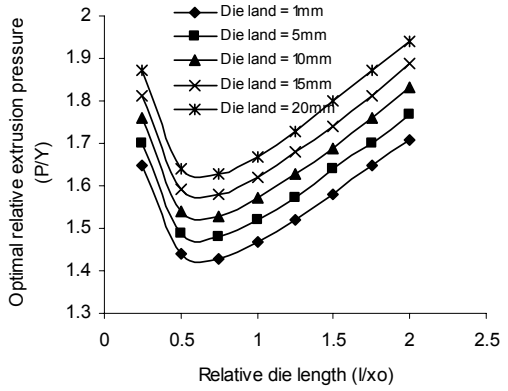


Fig. 6. Effects of die land lengths on the extrusion pressures of square die opening at a given die reduction in area of 58%.

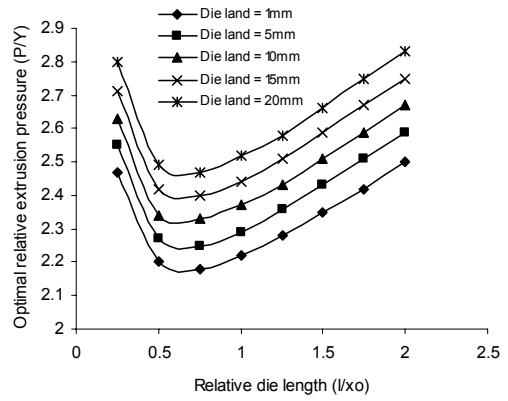


Fig. 7. Effects of die land lengths on the extrusion pressures of rectangular die opening at a given die reduction in area of 58%.

reached; beyond this minimum relative length, relative extrusion pressures start to increase again. The normalized extrusion pressure, $P_{min}/Y$, which corresponds to this minimum relative extrusion pressure gives the optimal extrusion pressure, $P_{min}/Y$, that is required to extrude under a given die land length for a given percentage reduction in area under consideration. It can be seen that, increasing the die land lengths will produce various optimal relative extrusion pressures irrespective of die opening's geometry (see Figs. 5, 6 and 7). Also, from Figs. 5, 6 and 7 using the same friction coefficient of 0.065 and percentage reduction in area of 58, the optimal relative die lengths are found to occur at the same points, i.e., $l/x_o$ = 0.75 for circular, square and rectangular die openings respectively, for all various die land lengths considered. This is in close agreement with Chitkara and Celik's [2] findings in their analytical models on the extrusion of T-section shape that for a particular friction factor. The optimal die length changed only slightly provided the reduction in cross-section area was either the same or close to each other. For other varying percentage reductions in area, R say 69% and 76%, the optimal relative die lengths are found to occur at $l/x_o$ = 0.5, respectively, for square die opening and at the same values of reduction in areas of 69% and 76%, the optimal relative die lengths are $l/x_o$ = 0.75 respectively for rectangular die opening.

### *5.2 Variation of normalized extrusion pressure with relative die land length*

#### *5.2.1 Square, rectangular and circular die openings*

Figs. 8, 9 and 10 show the theoretical plots of normalized extrusion pressure, $P'/Y$ versus normalized or relative die land lengths, $x/H_o$, for the respective square, rectangular and circular sections openings computed for varying percentages reductions in area indicated. Increasing the percentages reductions in area leads to increasing normalized extrusion pressures, $P'/Y$, for any given die land lengths and also that, increasing die land lengths leads to increasing normalized extrusion pressure at any given percentage reduction in area investigated. By repeating similar procedures, the optimum extrusion pressures are determined for other varying die land lengths, say 1 mm, 5 mm, etc at a given percentage reduction in area for the respective circular, square and rectangular sections openings of Figs. 5, 6 and 7. The

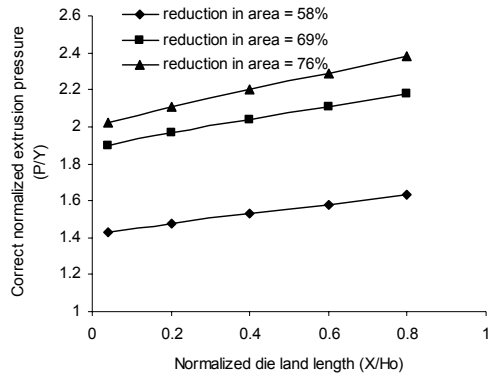


Fig. 8. Effects of die reduction in areas on the correct normalized extrusion pressures of square die opening.

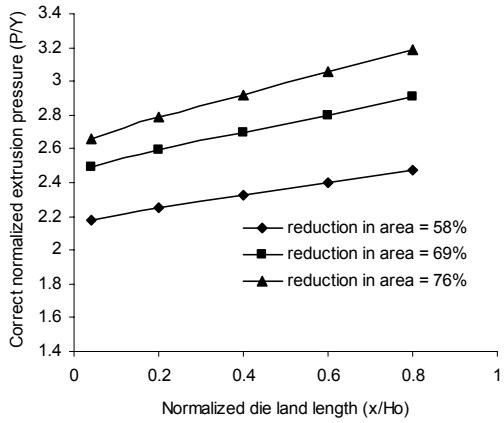


Fig. 9. Effects of die reduction in areas on the correct normalized extrusion pressures of rectangular die opening.

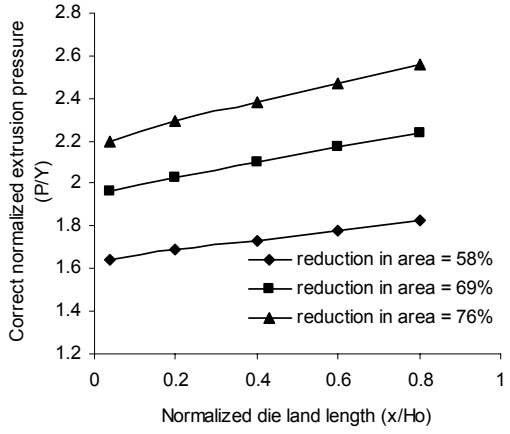


Fig. 10. Effects of die reduction in areas on the correct normalized extrusion pressures of circular die opening.

whole procedures are repeated at varying die land lengths and percentages reductions in area to give Figs. 8, 9 and 10 for the respective square, rectangular and circular die openings.

### *5.2.2 Die land length and die geometries extrusion pressure contributions, $\Delta P_o/Y$, Determination*

Extrapolating each plot of Figs. 8, 9 and 10 to intercept the extrusion pressure axis, gives the values of normalized extrusion pressure, $P_o/Y$, corresponding to zero die land length for each reduction in area indicated. For each given reduction in area, this value subtracted from the correct normalized extrusion pressure value, $P'/Y$, obtained for various die land lengths gives the extrusion pressure contribution of each die land length to the extrusion pressure as $\Delta P_o/Y = (P'-P_o)/Y$. The dimensionless die land length extrusion pressure contribution, $\Delta P_o/Y$, is seen to generally increase with increase die land lengths and also to increase with increased percentages reductions in area (see Table 1) for all die opening geometries investigated. Generally, die land lengths contribute significantly to the extrusion pressures for all die openings geometries and more especially at higher die reductions for any die opening geometry. Higher perimeters of these geometries coupled with higher frictional effects may possibly account for the higher contributions of die land lengths to the total extrusion pressures (see Table 1)

Fig. 11 shows the plot of the correct relative extrusion pressure, P/Y, versus increasing relative die land lengths at a given die reduction of 58% for

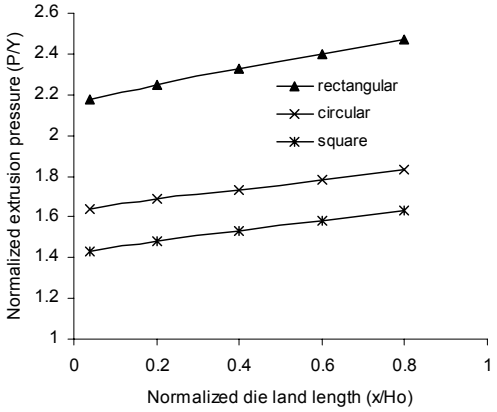


Fig. 11. Effect of die opening shape on the optimal relative extrusion pressure at a given die reduction in area of 58%.

Table 1. Die land extrusion pressure contributions, $\Delta P_o/Y$, at various % reductions in area for various die opening's profiles.

| Die opening geometry | %reduction in area, R | Extrapolated extrusion pressure $(P_o/Y)MNm^{-2}$ | Die land length contribution to extrusion pressure $\Delta P_o/Y$ | | | | |
|---|---|---|---|---|---|---|---|
| | | | 1 mm | 5 mm | 10 mm | 15 mm | 20 mm |
| quare | 58 | 1.40 | 0.03 | 0.08 | 0.13 | 0.18 | 0.23 |
| | 69 | 1.86 | 0.04 | 0.11 | 0.18 | 0.25 | 0.32 |
| | 76 | 1.98 | 0.04 | 0.13 | 0.22 | 0.31 | 0.40 |
| Circular | 58 | 1.61 | 0.03 | 0.08 | 0.12 | 0.17 | 0.22 |
| | 69 | 1.98 | 0.04 | 0.11 | 0.18 | 0.25 | 0.32 |
| | 76 | 2.18 | 0.04 | 0.13 | 0.24 | 0.37 | 0.46 |
| Rectangular | 58 | 2.14 | 0.04 | 0.09 | 0.17 | 0.24 | 0.31 |
| | 69 | 2.40 | 0.09 | 0.19 | 0.30 | 0.40 | 0.51 |
| | 76 | 2.58 | 0.08 | 0.21 | 0.34 | 0.48 | 0.61 |

circular, rectangle and square shaped die openings. The rectangular-shaped section die opening gives the highest extrusion pressure, followed by circular shaped die openings with square section die opening, giving the least extrusion pressure for the given 58% die reduction at any given die land lengths.

## 6. Conclusion

Using square or rectangular billets and upper bound analysis, the effect of the die land lengths on the extrusion pressure is formulated in Cartesian coordinates system for shaped extruded sections such as square and rectangular with the power of deformation due to ironing effect at die land included. The extrusion pressure contributions due to the die land evaluated theoretically for shaped sections considered are found to increase with die land lengths for any given percentage reduction and also increase with increasing percentage die reductions at any given die land length. The effect of die land lengths on the extrusion pressures increase with increasing complexity of die openings geometry with rectangular section giving the highest extrusion pressure followed by circular with square section die opening, giving the least extrusion pressure for any given die reduction at any given die land lengths. With adequate knowledge of the importance of friction in metal forming, the present 3-D rectangular coordinate formulation gave more convincing results to researchers in metal forming processes than the previous 2-D polar coordinate formulation [25].

## Acknowledgment

The author profoundly acknowledges the support by the Brain Korea 21 Project for postdoctoral research Program.

## Nomenclature

$J^*$ : Total power of deformation
$W_i$ : Internal strain rate power of deformation
$W_f$ : Frictional power losses
$W_s$ : Shear power dissipated at boundaries of velocity discontinuity.
$y^/$ : Current billet height to die surface
l : Length of die
$x_o$ : Original length of billet
x, y, z : Cartesian co-ordinate
$V_o$ : Steady punch velocity
$V_r, V_y, V_z$ : Velocity components.
$z_s(x, y)$ : Functions defining the shape of die geometry
$x_f(y)$ : Function defining the zone of plastic deformation
m : Friction coefficient
$P_{ave}$ : Average punch pressure
$\Delta v$ : Resultant velocity
$H_o$ : Original billet height
$y_1$ : Die length
R : % reduction in area
x : Die land length
$P_{max}, P_{min}, P^/$ : Extrusion pressures
Y : Mean yield stress
$A_2/A_1$ : Area ratio
a, b : Height, length of sides of rectangle section
$A_o$ : Original billet area
$A_1$ : Billet area responsible for the flange
$A_2$ : Billet area responsible for the web

### *Greek symbols*

$\sigma_o$ : Flow stress of the working material
$\Gamma_s$ : Boundaries of velocity
$\dot{\varepsilon}_{ii}, \dot{\varepsilon}_{ij}$ : Strain rate components discontinuity at

exit and entry

ε : True strain entry including singular points

## Reference:


[1] C. T. Yang, The upper-Bound Solution as Applied to Three-Dimensional Extrusion and Piercing Problems, *Trans. ASME Journal of Engineering for industry,* (1962) 397-403.

[2] N. R. Chitkara and M. A. Bhutta, Computer simulation to predict stresses, working pressures and deformation modes in incremental forging of spur gear forms, *International Journal of Mechanical Sciences,* 38 (1996) 871-889.

[3] N. R. Chitkara and Kim Yohngjo, Upper bound analysis of Near-Net shaped forging of gear coupling form, *International Journal of Mechanical Sciences,* 38 (1996) 791-803.

[4] J. C. Choi, Y. Choi and S. J. Tak, The forging of helical gears (1): Experiments and Upper-Bound analysis, *International Journal of Mechanical Sciences,* 40 (1998) 325-337.

[5] S. K. Sahoo and P. K. Kar, Round-to-hexagon drawing through straightly converging dies: an application of the SERR technique, *International Journal of Mechanical Sciences,* 42 (2000) 445-449.

[6] D. Y. Yang and H. S. Lee, Analysis of Three-Dimensional Deep Drawing by the Energy Method, *International Journal of Mechanical Sciences,* 35 (1993) 491-516.

[7] V. Nagpal and T. Altan, Analysis of the three-dimensional flow in extrusion of shapes with the use of dual stream functions, *Proceedings of the Third North American Metalworking Research Conference*, (1975) 26-40.

[8] D. Y. Yang and C. H. Lee, Analysis of three-dimensional extrusion of sections through curved dies by conformal transformation, *International Journal of Mechanical Sciences,* 20 (1978) 541-552.

[9] C. W. Wu and R. Q. Hsu, Theoretical analysis of extrusion of rectangular, hexagonal and octagonal composite clad rods, *International Journal of Mechanical Sciences,* 42 (2000) 473-486.

[10] W. B. Bae and D. Y. Yang, An upper-bound analysis of the backward extrusion of internally elliptic-shaped tubes from round billets, *Journal of Materials Processing Technology,* 30 (1992) 13-30.

[11] V. Nagpal, On the solution of three-dimensional metal-forming process, *Trans. ASME, ser.B*, 99 (1977) 624.

[12] D. Y. Yang and C. H. Han, Backward extrusion of internally shaped tubes from round billets, *Trans. ASME ser. B*, 106 (1984) 143.

[13] Y. H. Kim and J.H. Park, Upper bound analysis of torsional backward extrusion process, *Journal of Materials Processing Technology,* 143 – 144 (2003) 735-740.

[14] Y. H. Kim, Y. E. Park and Y. E. Jin, An analysis of plastic deformation processes for twist-assisted upset forging of cylindrical billets, *in: Proceedings of the International Conference on Advances in Materials and Processing Technologies (AMPT'99) and 16th Annual Conference of the Irish Manufacturing Committee (IMC16),* 1 (1999) 79-86.

[15] Y. H. Kim, Y. E. Park and Y. E. Jin, An upper bound analysis for torsional upset forging of cylindrical billets, *in: Proceedings of the Sixth International Conference on Technology of Plasticity, Advanced Technology of Plasticity*, 2 (1999) 859-864.

[16] Y. H. Kim, J. H. Park, Y. E. Jin and Y. Lee, An analysis of the torsional forming process using the dual stream function, *in: Proceedings of the Eight International Conference on Metal Forming, Metal Forming* 2000, (2000) 741-746.

[17] F. Gatto and A. Giarda, The characteristics of the three-dimensional analysis of plastic deformation according to the SERR method, *International Journal of Mechanical Science,* 23 (1981) 129-148.

[18] P. K. Kar and N. S. Das, Upper bound analysis of extrusion of I-section bars from square/rectangular billets through square dies, *International Journal of Mechanical Sciences,* 39 (1997) 925-934.

[19] N. R. Chitkara and M. B, Adeyemi, Working pressure and deformation modes in forward extrusion of I and T shaped sections from square slugs, *18th int. M. T. D. R Conf. Proceedings, Imperial College of science and Tech. London,* (1977) 289-301.

[20] C. T. Yang, On the Mechanics of Wire Drawing,. *Transactions of the ASME; Journal of Engineering for Industry,* (1961) 523-530.

[21] M. Kiuchi, H. Kish and M. Ishikawa, Study on Non symmetric extrusion and drawing, *Int. Journal Mach. Tool, Design and Research Conf. 22nd proceedings,* (1981) 523-532.

[22] Nanhai et al Numerical design of die land for shape extrusion, Journal *of Material Processing Technology,* 101 (2000) 81-84.

[23] J. S. Ajiboye and M. B. Adeyemi, Effects of Die land on the cold extrusion of lead alloy, *Journal of Materials Processing Technology,* 171 (2006) 428-

436.

[24] B. Avitzur, Analysis of Wire Drawing and Extrusion through Conical Dies of Small Cone Angle,. *Transactions of the ASME; Journal of Engineering for Industry,* (1963) 89-96.

[25] J. S. Ajiboye and M. B. Adeyemi, Upper Bound Analysis for Extrusion at Various Die Land Lengths and Shaped Profiles, *International Journal of Mechanical Sciences,* 49 (2007) 335-351.

[26] N. R. Chitkara and K. F. Celik, Extrusion of non-symmetric T-shaped sections an analysis and some experiments, *International Journal of Mechanical Sciences,* 43 (2001) 2961-2987.

**Ajiboye, Joseph S.** received his B.Eng, M.Eng, and PhD degrees in Mechanical Engineering from the University of Ilorin, Nigeria, in 1988, 1995 and 2006 res-pectively. Dr. Ajiboye is a lecturer in the Department of Mechanical Engineering, Uni-versity of Lagos, Nigeria. He is currently a Contract Research Scientist at KAIST Valufacture Institute of Mechanical Engineering, School of Mechanical, Aerospace & Systems Engineering, Korea Advanced Institute of Science and Technology, Daejeon 305 – 701, Korea. **Dr. Ajiboye's** research interests include ECAE/P, determination of frictional effects in metal forming operations, upper bound and finite element in plasticity.